Springer

KSME

Journal of Mechanical Science and Technology 28 (5) (2014) 1917~1925
www.springerlink.com/content/1738-494x
DOI 10.1007/s12206-014-0339-4

# An analysis of carbone monoxide distribution in large tunnel fires †

Atta Sojoudi, Hossein Afshin* and Bijan Farhanieh

*Center of Excellence in Energy Conversion, School of Mechanical Engineering, Sharif University of Technology, P. O. Box 11365-9567, Tehran, Iran*

(Manuscript Received May 22, 2013; Revised January 9, 2014; Accepted February 3, 2014)

**Abstract**

Fire events and the related toxicants such as CO are responsible for many fatalities in the current century. These hazardous events are much more dangerous when they occur in enclosed spaces. In the present study, a theoretical relation is developed for horizontal distribution of CO in a large tunnel fire. Then, the developed criterion is used to study the effect of some rudimentary parameters such as the heat release rate (*HRR*) of fire and tunnel's aspect ratio (*AR*) on CO and temperature stratification. Theoretical results of various heat release rates and aspect ratios for horizontal distribution of CO are compared with numerical results using fire dynamics simulator (FDS5.5). It is found that big fires have higher rates of CO concentration decay in comparison to the smaller ones due to higher air entrainment into the travelling plume. It is indicated that the smoke travelling at higher values of tunnel *AR*, dilutes faster. Moreover, using FDS5.5, the relevant variations in temperature and CO concentration are discussed for tunnel angles ranging from -20˚ to 20˚.

*Keywords*: Carbone monoxide distribution; CO and temperature stratification; FDS; Large tunnel fires

## 1. Introduction

Tunnel fires are related to toxicity and high temperature which are responsible for much of the tunnel fire mortality in recent decades. Mont-Blanc, in the France/Italy mountains on the morning of 24th of March 1999, 39 people were killed ; Daegu subway, Korea on 18th of February, 2003, 198 people were killed; St. Gotthard Tunnel in Switzerland on 24th of October 2001,11 people were killed and many other instances have also occurred which have attracted lots of researchers to tunnel fire safety [1-3]. One of the most significant issues in fire science is smoke movement and its related toxicity. It is important to note that inhaling toxic gases such as the Carbon monoxide released from fire is responsible for 75% to 85% of all casualties in tunnel fires [4], so toxicants such as CO rather than temperature are the reason for most fatalities in fire events. Therefore, appropriate techniques should be employed to remove smoke in tunnel fires.

In an earlier study, an experimental study was carried out by Newman [5] using a longitudinally ventilated horizontal mine passage and indicated that vertical profiles of temperature and CO concentration follow each other. Zhang et al. [6] studied the vertical and horizontal distributions of CO using a ¼-scaled rectangular model of tunnel fire. Their results showed that the maximum CO concentration decreased along the tunnel and the related delaying time decreased with the increase of velocity. Hu et al. [7] studied the influence of longitudinal ventilation velocity on the vertical difference of CO and temperature fields employing FDS5.5 (fire dynamics simulator) for a tunnel fire of 600m length × 10m width × 7m height. Their results indicated that the vertical profile differences of CO concentration and smoke temperature adjacent to ceiling decreased with the increase of longitudinal ventilation velocity. They also showed that the vertical profile of CO concentration dilutes faster than smoke temperature downwardly. Then, they used this numerical simulation [8] to study the horizontal distribution of CO and temperature fields near the ceiling, where one-dimensional approximation of smoke flow may be regarded as reasonable downstream of the fire. Smoke temperature was shown to decrease faster than CO concentration along the tunnel reaching an asymptotic value.

In recent studies, Yang et al. [9, 10] carried out a series of experiments to investigate the influence of longitudinal ventilation velocity on Carbon monoxide and thermal stratification. They [10] showed that the temperature of smoke decreases with the increase of distance apart from the fire while Carbon monoxide concentration remains unchanged along the tunnel. However, ventilation velocity had a negligible effect on the longitudinal dimensionless CO concentration. It means that fresh air entrainment into the smoke flow was also negligible during the experiment while CO concentration decay has been documented in former studies [8, 11]. This contradiction will be clarified when the amount of heat release rate is taken into account in tunnel fires. In other words, air entrainment may be considerable for big fires compared with small fires.

*Corresponding author. Tel.: +98 2166165530, Fax.: +98 2166000021
E-mail address: afshin@sharif.edu
† Recommended by Associate Editor Jun Sang Park

The smoke flow of inclined tunnels has been investigated through numerical simulations of computational fluid dynamics [12-14]. The main objective of those works was to determine the critical velocity for suppressing smoke's spreading in inclined tunnels. Nevertheless, since the CO gas is the main cause of death, it is urgent to study the buoyancy's effect on thermal and CO stratifications. Zhang et al. [15] used their previous experimental setup [9] to investigate the effect of non-ventilated tunnel fire inclination on CO generation for angles varying from -10˚ to 10˚. It was found that CO concentration decreases for specified probes downstream the fire with the increase of angle which denotes a high rate of mass loss in fuel. They didn't discuss the effect of inclination on the spatial distribution of CO [6]. According to the knowledge of authors, due to the serious hazards of Carbon monoxide aspiration, further investigations are needed to complete the information on CO spread in tunnel fires.

In a general view, the paper firstly deals with the theoretical relations previously obtained and gathers them to obtain a relationship between the important parameters of tunnel fire (such as tunnel geometry or heat release rate of fire, etc.) and the related pattern of Carbon monoxide distribution. Then, this relation is compared with the numerical and experimental works of Hu et al for various *HRRs* [8 and 16] to ensure the accuracy of the derived criterion. This comparison attributes to the horizontal distribution of CO beneath the ceiling. After that, we use our derived relation to estimate the horizontal distribution of CO for various tunnel aspect ratios. But there are limited studies in the literature to ensure our relation's accuracy in various aspect ratios. So our FDS5.5 results helped us to compare both the theoretical calculations for various aspect ratios and the numerical results. As a complementary work, the inclination effect was also studied and our relation seemed to deviate from the precise results of FDS5.5 for both horizontal and vertical distributions (some modifications should be applied to the relation to obtain good results for different slopes which will be presented in future works.). Here we relied on FDS5.5, because it has showed its great accuracy in other previous works of scientific investigation.

## 2. The theoretical analysis of smoke flow

In tunnel fires, a buoyancy-driven smoke flow forms beneath the ceiling. The smoke flow of tunnel / channel fire is described as below [17]:

(1) The impinging region of ascending plume on the ceiling;

(2) The radial spread of smoke;

(3) The transition stage to one-dimensional flow with interaction to the side walls;

(4) The final 1D spread of smoke.

This analytical study does not include the earlier stages of 1 to 3 because of high temperature, oxidation of CO and multi-dimensionality of the flow. The main objective of this analysis is to obtain a theoretical relation for the horizontal distribution of CO concentration and the related difference with thermal stratification through the tunnel ceiling for various *HRR*s and aspect ratios at stage 4. The model considers a burning object at the mentioned place assuming a longitudinal forced flow of ambient air. The schematic view of the tunnel and the specified control volume through which smoke enters and leaves, is depicted in Fig. 1. The control volume (C.V.) starts far enough downstream the fire up to the end of the tunnel, and the height of C.V. is almost the thickness of the smoke traveling beneath the ceiling (the C.V. width equals the tunnel width). Although the plume entering the C.V contains a small amount of fresh air, we assume that it is pure smoke. But then, as shown in Fig. 1, CO concentration is diluted through the air entrainment in the C.V.

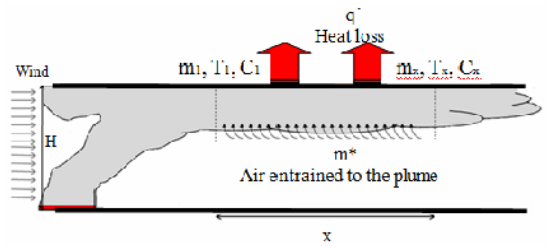


Fig. 1. Schematic view of the control volume.

Some assumptions based on which the theoretical relation is derived include the following:

(1) Steady state analysis [8-10];

(2) One-dimensional study of smoke flow [9, 12, 17];

(3) The uniform value of CO concentration and temperature at every cross-section of the C.V.;

(4) The main heat loss to the ambient is done through ceiling and other walls and floor can be rather insulated, but they receive radiative heat loss from the travelling smoke [17];

(5) Forced ventilation produces an air flow parallel to the axis of the tunnel and it drives the smoke to one side of the fire (the present analysis considers that side of the fire to which smoke moves, i.e. downstream);

(6) The C.V. inlet is far enough to contain any chemical reaction or multi-dimensionality of flow [8, 12, 17];

(7) The C.V length is assumed to be $x$ which can be extended to the end of the tunnel [8];

(8) The amount of CO mass entering the control volume is conserved [8];

(9) The smoke layer thickness is constant along the tunnel [18-20];

(10) Although the ventilation velocity has a significant effect on the amount of heat release rate (*HRR*), we assume that this influence of velocity has been applied to the value of *HRR* before assuaging the steady state condition, and then *HRR* is fixed. Some other assumptions are mentioned through deriving the relation as follows [8]. The mass conservation of CO, the energy balance for the control volume and the amount of mass entrained into the plume can be taken as [8]:

$$C_1 m_1 = C_x m_x$$
$$m_x = m_1 + m^* \quad (1)$$

$$c_p m_1 T_1 + c_p m^* T_a = c_p (m_1 + m^*) T_x + \dot{q} \quad (2)$$

$$m^* = \rho_a \beta w |u - u_s| x. \quad (3)$$

Eq. (1) shows the mass balance of CO between the inlet and the outlet of the control volume where $C_1$ and $C_x$ are the flow rates of CO in Kg/s per flow rate of smoke in Kg/s at the reference point and a point at position $x$ downstream of the reference position. $m_1$ and $m_x$ are local mass flow rates of smoke flow entering and leaving the C.V. respectively, and $m^*$ is the mass flow rate entrained into the C.V. Eq. (2) relates the energy entering and leaving the control volume. $T_a$ is the ambient temperature of the fresh air and $c_p$ is the specific heat capacity of gas. $\dot{q}$ is the rate of heat transfer to the ceiling from the reference point to position $x$ apart from the fire. Eq. (3) denotes the fresh air entrainment into the plume which is described by Kunsch [18]. $\rho_a$, $u$, $u_s$, $w$ and $\beta$ are ambient fresh air density, longitudinal ventilation air flow velocity, the travelling velocity of the smoke layer, the width of the tunnel and the entrainment coefficient, respectively. Re-arranging Eqs. (1) and (2), we find (by dividing Eq. (2) by $m_1$+$m^*$):

$$\begin{aligned} &c_P T_1 \left(\frac{C_x}{C_1}\right) + c_P T_a \left(1 - \frac{C_x}{C1}\right) = c_P T_x + \frac{\dot{q}}{m_1 + m^*} \\ &c_P (T_1 - T_a)\frac{C_x}{C_1} = c_P (T_x - T_a) + \frac{\dot{q}}{m_1 + m^*} \\ &\frac{C_x}{C_1} - \frac{\Delta T_x}{\Delta T_1} = \frac{\dot{q}}{c_p \Delta T_1 (m_1 + m^*)}. \end{aligned} \quad (4)$$

$\Delta T_x$ shows the temperature difference of the ambient air and location $x$ and $\Delta T_1$ indicates the temperature difference of ambient air and the C. V. inlet. For the rate of heat loss to the ceiling, we can write:

$$\dot{q} = \int_0^x \bar{h} P \Delta T_x dx, \quad (5)$$

in which $\bar{h}$ and $P$ show the average heat transfer coefficient and the perimeter of tunnel cross section adjacent to smoke, respectively. $\Delta T_x$ is shown to decay exponentially with $x$ [16, 17], where the radiation heat transfer to side walls has been taken into account within the definition of $\bar{h}$ .

$$\begin{aligned} &\frac{\Delta T_x}{\Delta T_1} = e^{-kx} \\ &k = \frac{\bar{h} P}{c_p m_1}. \end{aligned} \quad (6)$$

Using Eq. (6), Eq. (5) is written as:

$$\dot{q} = \bar{h} P \Delta T_1 \int_0^x e^{-kx} dx. \quad (7)$$

$\bar{h}P$ is supposed to be invariant with respect to $x$ [17, 21]. Using Eq. (7), Eq. (4) can be written as:

$$\frac{C_x}{C_1} - \frac{\Delta T_x}{\Delta T_1} = \frac{m_1 \left(1 - e^{-kx}\right)}{(m_1 + m^*)}. \quad (8)$$

Here we describe $m_1$ which is the mass inlet of smoke flow. We have:

$$m_1 = \rho_s u_s H_s, \quad (9)$$

where $\rho_s$, $u_s$ and $H_s$ present smoke flow density, smoke traveling velocity and the thickness of the plume, respectively. It is not far from the real tunnel fire characteristics to put the smoke flow density of the reference position equal to pure smoke density. Using Eqs. (3) and (9), Eq. (8) leads to the following expression:

$$\frac{C_x}{C_1} - \frac{\Delta T_x}{\Delta T_1} = \frac{\left(1 - e^{-kx}\right)}{1 + \left(\frac{\rho_a}{\rho_s}\right)\left(\left|\frac{u}{u_s} - 1\right|\right) x\beta / H_s}. \quad (10)$$

All the parameters related to tunnel fire characteristics on the right hand side of Eq. (10) should be found to derive the difference of CO and thermal stratification as a function of $x$ near the ceiling. The ratio of fresh air density to smoke density was obtained by Kunsch [18].

$$\frac{\rho_s}{\rho_a} = 1 - \frac{\alpha B^2}{gH}\left[1 + \left(\frac{\alpha B^2}{gH}\right)\right]^{-1} \quad (11)$$

where

$$\alpha = 6.13\left(\frac{w}{H}\right)^{2/3} \quad \& \quad B = \left(\frac{QgH}{c_p T_a \rho_a A}\right)^{1/3}.$$

$\alpha$ is the coefficient which will help to investigate the influence of aspect ratio on CO decay profile, $B$ is the buoyancy factor and $Q$ and $A$ are heat release rates of fire and the cross section area of tunnel, respectively.

For the ratio of velocities in the denominator of Eq. (10), we used the relation obtained by Zhang et al. [19] :

$$\frac{u_s}{u} = \frac{Z/L}{h_a/h_f + Z/L} \quad (12)$$

where $L$ is flame length, $h_a$ is fresh air enthalpy, $h_f$ is flame enthalpy and $Z$ denotes the average height of the smoke flow from the floor to the depth of the smoke layer.

$$L = \frac{Q}{\rho_a u h_a w}, \; h_a = c_p T_a, \; h_f = c_p T_f = c_p T_{\max}$$

$\beta$ in Eq. (10) is a small factor [17, 18] known as the air entrainment factor. The only unknown factor is the smoke layer thickness which is assumed to be constant for the region of study. This height is difficult to measure analytically, but Kunsch [18] has described an ancient measurement for that which is almost 5 to 10 percent of the tunnel height. It can be assumed that Eq. (10) has the simpler form than Eq. (13), with two distinct constants, namely $k$ and $b$ representing smoke temperature decay and CO concentration decay factors, respectively. Eq. (10) may be written in the simpler form of Eq. (13) using Eqs. (6), (11), (12):

$$\frac{C_x}{C_1}-\frac{\Delta T_x}{\Delta T_1}=\frac{1-e^{-kx}}{1+bx}. \tag{13}$$

In this Eq. $k$ and $b$ represent smoke temperature decay and CO concentration decay factors, respectively, and are determined via fire and tunnel characteristics. It is notable that the amount of heat loss is represented by the longitudinal decay rate exponent, $k$. It is also concluded that $k$ is adversely related to the mass flow rate. A larger ventilation velocity gives larger mass flow rate which results in smaller heat loss exponent, $k$ (See Eq. (6)).

### *2.1 The effect of HRR on CO distribution*

This part is devoted to investigating the effects of *HRR* value on the constants of Eq. (13); $b$ and $k$. These parameters should be analyzed to obtain the influence of *HRR* value on CO distribution. According to our assumption in Sec. 2 (see number 10), *HRR* is fixed in this analysis. Using Eq. (10), $b$ is:

$$b=\left(\frac{\rho_a}{\rho_s}\right)\left(\left|\frac{u}{u_s}-1\right|\right)\Big/H_s. \tag{14}$$

Density ratio is related to *HRR* through Eq. (11) as below:

$$\frac{\rho_a-\rho_s}{\rho_s}\propto Q^{2/3}. \tag{15}$$

Velocity ratio dependence on *HRR* is determined via Eq. (12). Simplifying this Equation, we find:

$$\frac{u_s}{u}=\frac{\dfrac{H\rho_a u h_a w}{Q}}{\dfrac{T_a}{T_f}+\dfrac{H\rho_a u h_a w}{Q}}. \tag{16}$$

An order of magnitude between the two terms of the denominators of Eq. (16) for a fire scenario of 4 MW *HRR* and 1m/s ventilation velocity reveals that:

$$\frac{\dfrac{T_a}{T_f}}{\dfrac{H\rho_a u h_a w}{Q}}\approx 0.01.$$

This means, velocity ratio is nearly unity for the above case and the ratio of smoke to fresh air velocity will be 1.019. Similarly, for 10 MW and 1m/s ventilation it will be 1.0185 which shows an approximate independence of velocity ratios on *HRR*. $H_s$ is assumed to be constant for the range of *HRR* used in this analysis [17, 21]. The entrainment factor, $\beta$, can be further analyzed to impose the *HRR* effect, but to make the analysis simpler, it is taken constant (an average value of $\beta$ is used for the studied *HRR*s [17]).

$k$ which is defined as the constant exponent of the exponential decay of temperature along the tunnel, has been studied through many researches [17, 22-24]. The parameter $k$ is the function of $m_1$, $\bar{h}$, $c_p$ and $P$ among which the last two are independent of *HRR*. A higher heat release rate reinforces the buoyancy-driven flow and enhances the average temperature in the tunnel. The specific heat is not a strong function of the temperature and may exist in the domain [17]; also the configuration of smoke is not altered significantly to vary the perimeter. So we assume the last two parameters as constant numbers of an average value for the range of temperature through the tunnel. Drysdale [25] has introduced smoke flow rate as below:

$$m_1=0.071Q^{1/3}z^{5/3}\left[1+0.026Q^{2/3}z^{-5/3}\right]kg/s \tag{17}$$

where $Z$ shows the smoke layer's average height. Eq. (17) denotes the significant dependency of smoke flow rate on *HRR*. The heat transfer coefficient of smoke flow consists of two parts; the convective heat losses to the boundary surface and the radiative heat losses [17]:

$$\begin{aligned}&\bar{h}=h_c+h_r, && \text{for the smoke layer which touches the floor of the tunnel.}\\ &\bar{h}=h_c+h_r\frac{P+w}{w}, && \text{for the smoke layer which doesn't touch the floor of thetunnel.}\end{aligned} \tag{18}$$

where $h_c$ is the convective heat transfer coefficient and $h_r$ is the radiative heat transfer coefficient:

$$h_r=\varepsilon_e\sigma(T_s+T_a)(T_s^2+T_a^2) \tag{19}$$

$\varepsilon_e$ is emissivity, $\sigma$ is Boltzmann constant, $5.67\times10^{-11}$ kW/(m$^2$.K$^4$) and $T_s$ is the temperature of the boundary surface. Emissivity was taken as 0.7 as used formerly [26-28]. Hengdong has suggested a simple empirical relation for convective heat transfer coefficient [17, 29]:

$$h_c=2K'\sqrt{u_s} \tag{20}$$

where the constant $K'$ varies from 0.0058 to 0.01161 kJ/m$^2$.K.s and $u_s$ indicates the travelling velocity of the smoke layer. Using the second-order polynomial equation developed

Table 1. Comparison of representative values of *b* and *k* between present theoretical study and numerical investigation of Hu et al. [8] (Initial values for the numerical simulation: 2.5 m/s longitudinal ventilation velocity for the entire domain, Both portals are set to be open, amount of *HRR* for each scenario is almost constant, walls contain convective boundary condition with 25C°ambient air [8]).

| *HRR* (MW) | k (Hu et al. [8]) | k (theoretical model) | Difference in k (%) | b (Hu et al. [8]) | b (theoretical model) | Difference in b (%) |
|---|---|---|---|---|---|---|
| 4 | 0.002791 | 0.0028 | -0.32 | 0.002507 | 0.0023 | 8.25 |
| 10 | 0.003012 | 0.0029 | 3.71 | 0.002532 | 0.0026 | -2.68 |
| 20 | 0.003039 | 0.003 | 1.28 | 0.003561 | 0.0033 | 7.30 |

by Megret and Vauquelin [20], smoke temperature can be easily evaluated in various *HRR*s. Also, Eq. (17) is used to obtain the smoke's travelling velocity of Eq. (6).

### *2.2 The effect of aspect ratio on CO distribution*

The aspect ratio of a tunnel (its width to its height) varies while its cross-sectional area (*WH*) is assumed to be constant. Density ratio is related to *H* through Eq. (15). Eq. (16) shows that aspect ratio does not have an effect on velocity ratio because the value of *WH* is constant. Density ratio is related to *H* through Eq. (11) as follows:

$$\frac{\rho_a - \rho_s}{\rho_s} \propto H^{-5/3}. \tag{21}$$

Eq. (16) shows that aspect ratio does not have an effect on velocity ratio because the value of *WH* is constant. The smoke layer height directly depends on the tunnel height which can be conveniently evaluated [17]. The value of *P* in the constant *k* is determined using Eq. (19). The two side walls and the width of the tunnel are used to calculate the perimeter.

$$P = H(AR + 0.1). \tag{22}$$

Smoke flow rate and specific heat do not change by aspect ratio. The effect of aspect ratio on radiative and convective heat transfer coefficients is easily evaluated through Eqs. (19) and (20).The typical values of *b* and *k* are given in Table 1 for the fire scenarios studied in the paper. The values of the present theoretical criterion and the numerical results evaluated by Hu et al. [8] are compared.

## 3. Numerical simulation

The CFD tool, FDS5.5 (fire dynamics simulator) which is developed by the National Institute of Standards and Technology (NIST), is used in this study for numerical simulations [30, 31]. A full identification and validation of examples are available at Refs. [30-32]. The time-dependent group of Navier-Stokes equations for buoyant-driven fluid flow is solved numerically through modeling turbulence by the technique of large Eddy simulation (LES). It is second-order accurate in numerical space and time differences.

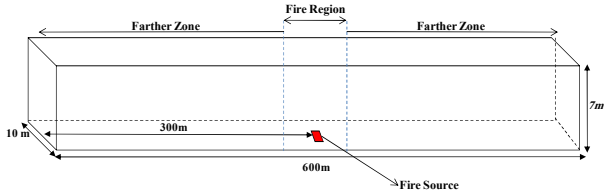


Fig. 2. Physical model for CFD simulation.

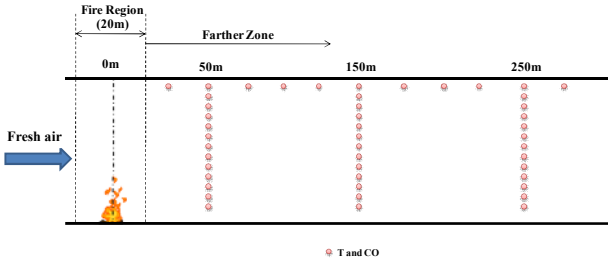


Fig. 3. Sample points used for CFD simulation.

A square Heptan pool fire is located in the middle of the tunnel and its heat output rate is known by heat release rate per unit area (The specified command "HRRPUA" provided by FDS5.5). The boundary material is set as concrete and the heat output of the pool fire is taken as 4, 10 and 20 MW. These values of *HRR* are related to an approximate heat release output of real cars, buses and trucks, respectively [8]. A road tunnel of 600 m × 7 m × 10 m (length×height × width) is assumed as described in [8] (see Fig. 2).

Both portals of the tunnel are adjusted to be open with no initial velocity. The longitudinal velocity is imposed on the entire domain of the computational domain initially. The tunnel walls are assumed to have the convective boundary condition in which the heat is transferred to the ambient air of 25C°. The sample points for measuring temperature and CO concentration are assigned as shown in Fig. 3. The longitudinal distribution of samples is set to be from 50 m downstream the fire to 250 m, at the intervals of 25 m located 25 cm beneath the ceiling. It is worthy of notice that the spread of the smoke comes to a one-dimensional flow in the near-the-ceiling samples and any complex chemical reaction can be ignored [8].

LES simulation is sensitive to grid size. Typically, smaller grid sizes can give detailed information, but they need much more computational time. Refining the mesh size increases accuracy, so the entire domain is divided into two distinct parts including the fire region and the farther zones. For a near-fire region grid size of 0.13 m (almost 7.7 cells in 1 m) and a coarser grid size of 0.4 m (2.5 cells in 1m) a good prediction can be obtained for real tunnel fires in FDS5.5 [33, 34]. For the present simulations, a distance of 0.125 m is regarded as near the fire (8 grids in 1 m) covering 10 m upstream and 10 m downstream the fire. All cells are cubic for near-the-fire region and other places. The grid size for the other places is

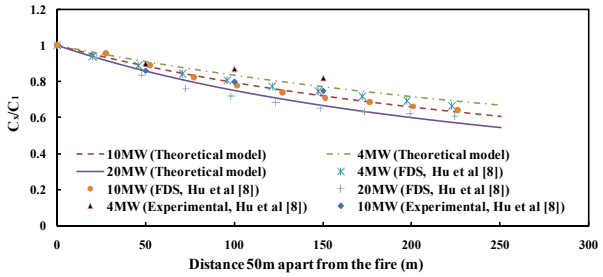


Fig. 4. *HRR* effect on horizontal distribution of CO (comparison of present theoretical study and results obtained by Hu et al. [8]).

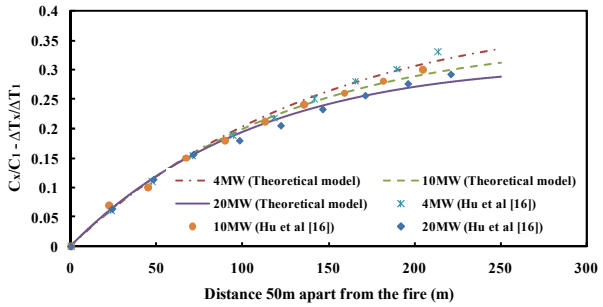


Fig. 5. *HRR* effect on horizontal distribution of CO and temperature difference (comparison of present theoretical study and results obtained by Hu et al. [8, 16]).

considered 0.333 m (3 grids in 1 m).

## 4. Results and discussion

In this part, results are presented in 3 distinct sections including the considerations of *HRR*, the effects of tunnel aspect ratio and tunnel inclination on Carbon Monoxide, and the thermal stratification. Each section consists of the horizontal profiles of the CO dimensionless volume concentration and its difference with the temperature field. The horizontal profiles are provided from 50 m to 250 m downstream the fire 25 cm below the ceiling, where the one-dimensional approach is used for analytical study. The horizontal values are normalized by the local value of the highest position at 50 m downstream the fire and 25 cm beneath the ceiling. The longitudinal ventilation velocity is supposed to be 2.5 m/s for the considerations on *HRR* and aspect ratio variations.

### *4.1 The consideration of HRR effect*

Not only a higher *HRR* increases the tunnel average temperature, but it also reinforces the buoyant-driven flow. In this section, our extended criterion is compared with those numerical and experimental results of Hu et al. [8, 16]. Fig. 4 makes a comparison between the present theoretical results of horizontal Carbon monoxide distribution, the FDS results obtained by Hu et al. [8] and a set of full scale experimental test by Hu et al. [16] for various *HRR*s. Note that experimental part were conducted in a road tunnel -Number 1 Road Tunnel of YuanJiang. The tunnel is located in the western part of China, being a key part of the highway systems between the cities Yuanjiang and Yuxi in the mountainous Yunnan Province, China [16]. The height and width of the mentioned tunnel are approximately 7 m and 10 m, respectively. As observable, a good agreement is reached between the theoretical and the results obtained by Hu et al. With an increase in *HRR*, the fresh air entrainment into the traveling smoke is enhanced. The dilution of smoke at a high *HRR* causes the CO to reduce faster than at a low *HRR*.

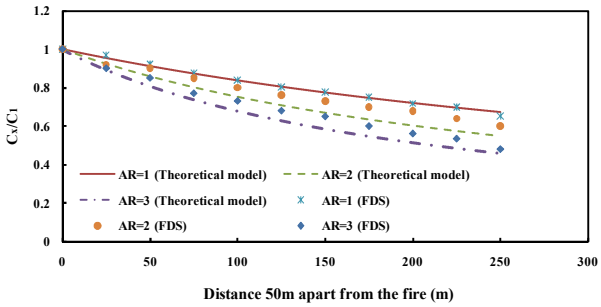


Fig. 6. Tunnel aspect ratio effect on CO horizontal dilution (comparison of present theoretical study and numerical results obtained by authors using FDS5.5).

Fig. 5 displays the present theoretical study and the numerical and experimental results of Hu et al. [8, 16] for the effect of *HRR* on the horizontal difference of CO and thermal stratification. At distances close to the fire, the temperature reduces faster than CO leading to the increment of CO and temperature difference, but then it reaches an asymptotic value for all *HRR*s. The heat transferred to the ceiling and the fresh air entrainment are two important mechanisms for temperature reduction. For the fire region, *HRR* value has no influence on CO and temperature difference. This shows the massive entrainment of fresh air at early distances, but farther distances include less air entrainment and the important mechanism of temperature reduction is convective heat transfer which is higher for big *HRR*s. So, big fires have less difference of CO and temperature for farther regions due to their higher heat transfer coefficient.

### *4.2 Considerations on tunnel aspect ratio*

Tunnel aspect ratio (*AR*), width to height of the tunnel, affects the smoke flow pattern in tunnel fires. In this study, the hydraulic diameter is kept constant for different ratios. In a narrow tunnel (low aspect ratio) the fire plume fills the whole part of the tunnel near the fire; therefore, less air is entrained into the smoke flow at short distances from the fire, but in a wide tunnel (with high aspect ratio) the vicinity of the fire will sense a great amount of fresh air due to the large free space available [35]. We report the analytically-estimated horizontal distribution of CO and temperature and compare them with our FDS5.5 simulations as there isn't sufficient information about it in the related literature. Fig. 6 shows a comparison of the present theoretical relation and the numerical results ob-

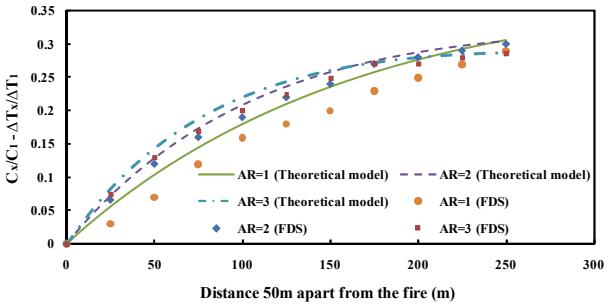


Fig. 7. Tunnel aspect ratio effect on CO and temperature horizontal difference (Comparison of present theoretical study and numerical results obtained by authors using FDS5.5).

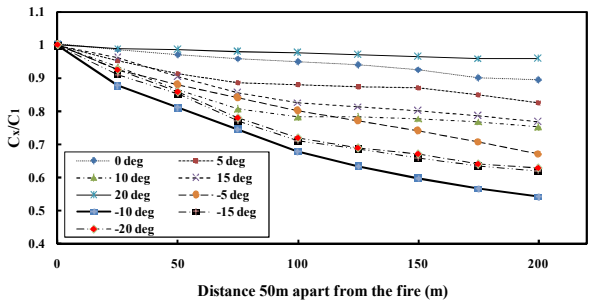


Fig. 8. Longitudinal distribution of CO for different slopes.

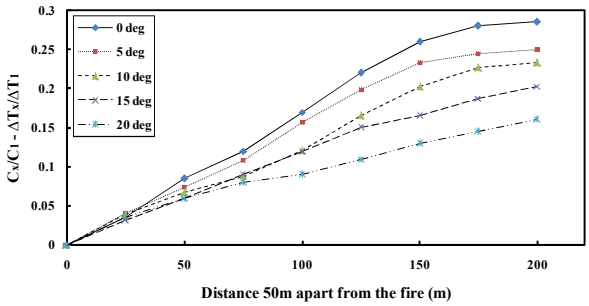


Fig. 9. Longitudinal distribution of CO and temperature stratification for different positive slopes.

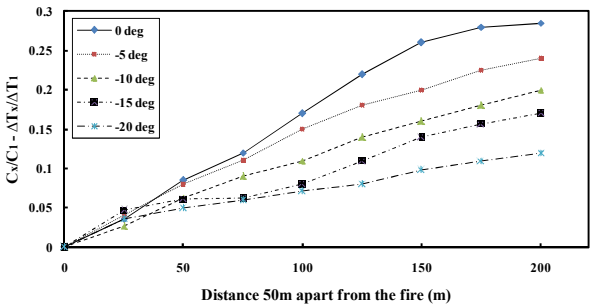


Fig. 10. Longitudinal distribution of CO and temperature stratification for different negative slopes.

tained by the authors using FDS5.5 (for more detailed information refer to the former sections) for the horizontal stratification of CO. A high *AR* of the tunnel makes the plume to be diluted faster. This denotes a massive air entrainment at near-the-fire region for higher aspect ratios leading to a faster decay of CO along the tunnel. Fig. 7 displays the difference of CO and temperature stratification for various tunnel aspect ratios evaluated by the theoretical relation and our FDS5.5 numerical results of the present study. For higher aspect ratios, the ceiling temperature reduces faster than CO concentration. As discussed above, the tunnel height is closer to the fire for *AR* = 3 which is responsible for the increased maximum temperature at this ratio. It has been shown that the temperature field decays faster at higher aspect ratios leading to an increase in the CO and temperature difference [36]. The rate of the temperature reduction is lowered by a decrease in the heat loss to the side directions as the ratio decreases and this makes the specified difference reach a similar asymptotic value.

### *4.3 Considerations on tunnel inclination*

Our theoretical criterion is incapable of describing horizontal profiles of CO and temperature. It needs some modification to be applicable to different slopes. So, we report our FDS5.5 results of various inclinations. In this part, CO and temperature profiles are investigated for a better conception of this fact. It should be noted that negatively inclined tunnel fires should include a higher value of longitudinal ventilation to prevent the back layered smoke; so, all test cases are studied by a 5 m/s longitudinal velocity for a 4MW fire [37]. Fig. 8 indicates the horizontal distribution of CO near the ceiling for different inclinations. As observable, for the inclinations of 5˚ and 10˚ CO concentration reduces faster with increasing the angle. Then it reaches a critical value for a slope of nearly 15˚ and reduces slower than at 10˚ until it reaches 20˚ which shows a higher concentration than an inclination of 0˚. Negative angles have the same variations. CO concentration reduces faster as the slope decreases to -10˚, and then it reaches a critical value between -10˚ and -15˚ angles. After the critical angle, it reduces slower, but less than that at 0˚. In fact, a slight increase in the angle, reinforces the buoyant flow in which in turn increases the travelling velocity of the smoke. This, somehow, enhances the fresh air entrainment into the plume, but after a critical angle value, the smoke flow accelerates further and the results of Ref. [8] for increasing the longitudinal velocity appear. With increasing the longitudinal velocity, CO decays slower due to the relatively less influence of inertial forces on air entrainment.

Figs. 9 and 10 show the horizontal distribution of thermal and CO stratification for positive and negative angles, respectively. With an increase in the positive angle or a decrease in the negative angle, the temperature reduces much faster than CO non-dimensional concentration. For distances close to the fire, the difference increases until it reaches an asymptotic value where the temperature is near the ambient temperature and no reduction of CO concentration is implemented. In other words, increasing or decreasing the tunnel inclination from the horizontal position, reduces the temperature much

faster than ever and this may be explained by the large contact of inclined tunnels with the ceiling surface resulting in more convective heat transfer.

## 5. Conclusions

A theoretical and numerical study of a large tunnel fire has been performed to investigate the relevant thermal and CO stratifications. The theoretical relations previously obtained were gathered and used to prepare a relationship between the important parameters of the tunnel fire (such as tunnel geometry or the heat release rate of fire, etc.) and related pattern for Carbon monoxide distribution. Then, this relation is compared with Hu's work for various *HRRs* [8, 16] to ensure the accuracy of the derived relation. This testing attributes to the horizontal distribution of CO beneath the ceiling. It has been shown that with increasing the *HRR*, the fresh air entrainment into the smoke plume increases and the CO concentration reduces faster. The difference of CO concentration and temperature increases for the distances close to the fire, then it reaches an asymptotic value which is higher in big fires. After that, we used our derived relation to estimate the horizontal distribution of CO at various tunnel aspect ratios. With an increase in aspect ratio, CO decays faster and the ceiling temperature reduces much faster due to the increment of ceiling convective heat transfer area. Tunnel inclination also influences the flow pattern. The reduction of tunnel angle resulted in enhancing the smoke layer showing no tilting for negative angles, but as the slope increased, the smoke flow tilted upward resulting in the reduction of smoke layer. Positive angles give a faster decay of CO concentration until the critical inclination of nearly 15˚, then the decay rate gets slower than even its rate at 0˚ when the angle reaches to 20˚. For negative slopes a similar pattern is seen as well.

## Nomenclature

$A$ : Cross section of tunnel [$m^2$]
$AR$ : Aspect ratio [-]
$B$ : Buoyancy factor [-]
$b$ : Decay factor of CO concentration [$m^{-1}$]
$c_p$ : Specific heat capacity [kJ/Kg.K]
$C_x$ : CO concentration at exit of control volume [-]
$C_1$ : CO concentration at enter of control volume [-]
$h_a$ : Fresh air enthalpy [kJ/Kg]
$h_f$ : Enthalpy of air at flame temperature [kJ/Kg]
$h_c$ : Convective heat transfer coefficient [$W/m^2.K$]
$h_r$ : Radiative heat transfer coefficient [$W/m^2.K$]
$hp$ : Average heat transfer coefficient [$W/m^2.K$]
$H_s$ : Smoke layer thickness [m]
$HRR$ : Heat release rate [W]
$H$ : Height of tunnel [m]
$K'$ : Constant ratio of convective heat transfer coefficient [$kJ/m^2.K.s$]
$k$ : Decay factor of smoke layer temperature [$m^{-1}$]
$L$ : Flame height [m]
$m_1$ : Mass flow rate of smoke layer at enter of control volume [kg/s]
$m_x$ : Mass flow rate of smoke layer at exit of control volume [kg/s]
$m^*$ : Air entrainment flow rate to the travelling smoke layer [kg/s]
$P$ : Perimeter of tunnel adjacent to smoke [m]
$q$ : Heat loss rate from smoke layer to the ceiling [W]
$Q$ : Heat released from fire [W]
$q_r$ : Radiative heat flux [$W/m^2$]
$T_f$ : Flame temperature [K]
$T_{max}$ : Maximum temperature of the flame [K]
$T_s$ : Inner surface temperature of tunnel [K]
$T_1$ : Smoke layer temperature at enter of control volume [K]
$T_a$ : Ambient air temperature [K]
$T_x$ : Smoke layer temperature at exit of control volume [K]
$t$ : Time [s]
$u$ : Longitudinal ventilation velocity [m/s]
$w$ : Width of tunnel [m]
$x$ : Distance 50m apart from fire source [m]
$Z$ : Smoke layer average height [m]
$\alpha$ : Geometric constant of tunnel [-]
$\beta$ : Entrainment coefficient [-]
$\varepsilon_e$ : Emissivity [-]
$\rho$ : Density [$kg/m^3$]
$\rho_a$ : Ambient air density [$kg/m^3$]
$\rho_s$ : Travelling smoke layer density [$kg/m^3$]
$\sigma$ : Boltzman constant [$kW/(m^2.K^4)$]

## References

[1] F. Vuilleumier, A. Weatherill and B. Crausaz, Safety aspects of railway and road tunnel: Example of the lotschberg railway tunnel and mont-blanc road tunnel, *Tunnelling and Underground Space Technology*, 17 (2002) 153-158.
[2] W. H. Hong, The progress and controlling situation of daegu subway fire disaster, *6th Asia-Oceania Symposium on Fire Science and Technology*, Daegu, Korea (2004) 28-46.
[3] Y. Huang, T. H. Hong and C. N. Kim, A numerical simulation of train-induced unsteady airflow in a tunnel of Seoul subway, *Journal of Mechanical Science and Technology*, 26 (3) (2012) 785-792.
[4] M. M. Hirschler, Smoke toxicity measurements made so that the results can be used for improved fire safety, *Journal of Fire Sciences*, 9 (4) (1991) 330-47.
[5] J. S. Newman, Experimental evaluation of fire-induced stratification, *Combustion and Flame*, 57 (1) (1984) 33-39.
[6] J. Zhang, Y. Lizhong, X. Qinkun and L. Xiao, Experimental study on CO distribution in the reduced-scale tunnel fire under longitudinal ventilation, *Journal of Applied Fire Science*, 20 (1) (2010) 1-19.
[7] L. H. Hu, D. Yang, Y. Q. Jiang, R. Huo and S. Liu, A com-

parative study on vertical profiles of smoke temperature and carbon monoxide concentration in a tunnel fire, *Journal of Applied Fire Science*, 17 (1) (2007) 21-35.

[8] L. H. Hu, F. Tang, D. Yang, S. Liu and R. Huo, Longitudinal distributions of CO concentration and difference with temperature field in a tunnel fire smoke flow, *International Journal of Heat and Mass Transfer*, 53 (13-14) (2010) 2844-855.

[9] D. Yang, R. Huo, X. l. Zhang, S. Zhu and X. Y. Zhao, Comparative study on carbon monoxide stratification and thermal stratification in a horizontal channel fire, *Building and Environment*, 49 (2012) 1-8.

[10] D. Yang, R. Huo, X. L. Zhang and X. Y. Zhao, Comparison of the distribution of carbon monoxide concentration and temperature rise in channel fires: reduced-scale experiments, *Applied Thermal Engineering*, 31 (4) (2011) 528-36.

[11] Y. Lizhong, F. Wenxing and Y. Junqi, Experimental research on the spatial distribution of toxic gases in the transport of fire smoke, *Journal of Fire Sciences*, 26 (1) (2008) 45-62.

[12] Y. Oka, Control of smoke flow in tunnel fires, *Fire Safety Journal*, 25 (4) (1995) 305-22.

[13] Y. Wu, H. J. Xing and G. T. Atkinson, 'Interaction of fire plume with inclined surface, *Fire Safety Journal*, 35 (2000) 391-403.

[14] C. Hwang and J. Edwards, The critical ventilation velocity in tunnel fires—a computer simulation, *Fire Safety Journal*, 40 (3) (2005) 213-44.

[15] J. Zhang, X. Zhou, Q. Xu and L. Yang, The inclination effect on CO generation and smoke movement in an inclined tunnel fire, *Tunnelling and Underground Space Technology*, 29 (2012) 78-84.

[16] L. H. Hu, R. Huo and W. K. Chow, Studies on buoyancy-driven back-layering flow in tunnel fires, *Experimental Thermal and Fluid Science*, 32 (8) (2008) 1468-1483.

[17] L. H. Hu, R. Huo, W. K. Chow, H. B. Wang and R. X. Yang, Decay Of buoyant smoke layer temperature along the longitudinal direction in tunnel fires, *Journal of Applied Fire Science*, 13 (1) (2004) 53-77.

[18] J. P. Kunsch, Critical velocity and range of a fire-gas plume in a ventilated tunnel, *Atmospheric Environment*, 33 (1999) 13-24.

[19] Q. Zhang, X. Guo, E. Trussoni, G. Astore, S. Xu and P. Grasso, Theoretical analysis on plane fire plume in a longitudinally ventilated tunnel, *Tunnelling and Underground Space Technology*, 30 (2012) 124-131.

[20] O. Megret and O. Vauquelin, A model to evaluate tunnel fire characteristics, *Fire Safety Journal*, 34 (2000) 393-401.

[21] L. H. Hu, R. Huo, H. Wang, Y. Li and R. Yang, Experimental studies on fire-induced buoyant smoke temperature distribution along tunnel ceiling, *Building and Environment*, 42 (11) (2007) 3905-915.

[22] M. Delichatsios, The flow of fire gases under a beamed ceiling, *Combustion and Flame*, 43 (1981) 1-10.

[23] C. Koslowski and V. Motevalli, Behavior of a 2-dimensional ceiling jet flow: A beamed ceiling configuration, *Fire Safety Science*, 4 (1994) 469-80.

[24] L. Li, X. Cheng, X. Wang and H. Zhang, Temperature distribution of fire-induced flow along tunnels under natural ventilation, *Journal of Fire Science*, 30 (2012) 122-137.

[25] D. Drysdale, *An introduction to fire dynamics*, Chichester, West Sussex: Wiley (2011).

[26] B. Karlsson and J. G. Quintiere, *Enclosure fire dynamics*, Boca Raton, FL: CRC (2000).

[27] D. Xilin, Z. Weifeng and Q. Lijun, The calculation of the safe unsealing time after suppressing the tunnel fire, *Fire Science and Technology*, 2 (1999) 4-7.

[28] D. Xilin and Y. Gaofeng, Oxygen-lacking combustion in tunnel fire, *Fire Science and Technology*, 4 (2000) 4-6.

[29] H. Hengdong, Variation of smoke temperature and smoke pressure and the corresponding fire protection engineering for underground fires, *Journal of Chongqing Institute of Architecture and Engineering*, 17 (1995) 68-73 (in Chinese).

[30] K. B. McGrattan and G. P. Forney, *Fire dynamics simulator (Version 4.07) - User's guide*, NIST Special Publication 1019, National Institute of Standards and Technology, Gaithersburg, MD (2006).

[31] M. Kevin, K. Bryan and H. Simo, *Fire dynamics simulator (Version 5) user's guide*, National Institute of Standards and Technology Special Publication (2007).

[32] P. A. Friday and F. W. Mowrer, Comparison of FDS model predictions with FM/SNL fire test data, *NISTGCR01-810*, National Institute of Standards and Technology, Gaithersburg, MD (2001).

[33] K. B. McGrattan and A. Hamins, Numerical simulation of the howard street tunnel fire, Baltimore, Maryland, July 2001. *NISTIR 6902*, National Institute of Standards and Technology, (2002).

[34] A. A. F. Peters and R. Weber, Mathematical modelling of a 2.25MW swirling natural gas flame, Part 1: Eddy break-up concept for turbulent combustion; probability density function approach for nitric oxide formation, *Combust. Sci. Tech*. 110-111 (1995) 67-101.

[35] O. Vauquelin and Y. Wu, Influence of tunnel width on longitudinal smoke control, *Fire Safety Journal*, 41 (6) (2006) 420-26.

[36] S. Lee and H. Ryou, A numerical study on smoke movement in longitudinal ventilation tunnel fires for different aspect ratio, *Building and Environment*, 41 (6) (2006) 719-25.

[37] *ASHRAE Han dbook*, Atlanta, GA: American Society of Heating, Refrigeratingand Air Conditioning Engineers (1998).

**Atta Sojoudi** received B.S. degree (with highest honors) from Tabriz University in 2012, and now is M.S.c student in the Mechanical Engineering Department at Sharif University of Technology (SUT) under the supervision of Professor Bijan Farhanieh. His research interests are numerical studies in fluid mechanics and heat and mass transfer.